PERGAMON

Radiation Measurements 32 (2000) 129–140

Radiation Measurements

www.elsevier.com/locate/radmeas

The interpretation of quartz optically stimulated luminescence equivalent dose versus time plots

Richard M. Bailey

Research Laboratory for Archaeology and the History of Art, University of Oxford, 6 Keble Road, Oxford, OX1 3Q1, UK

Received 5 May 1999; received in revised form 21 July 1999; accepted 18 September 1999

Abstract

Numerical modelling has shown that the form of the quartz OSL shine plateau (hereafter '$D_e(t)$-plot') is influenced by the effects of phototransferred TL in the ~110°C region. It is suggested also that the presence of multiple OSL components (as described by Bailey, Smith and Rhodes, 1997. Partial bleaching and the decay form characteristics of quartz OSL. Radiat. Meas., 27, 123–136; Bailey, 1998. The form of the optically stimulated luminescence signal of quartz: implications of dating. Unpublished PhD thesis, University of London) affects the form of the $D_e(t)$-plot. Laboratory measurements of a fully reset and artificially dosed sample yielded non-flat $D_e(t)$-plots, the deviation being greater for the larger of the two simulated palaeodoses, in accordance with theoretical predictions. It is suggested that the so-called 'shine plateau' test is of limited use in assessing the bleaching history of quartz sediments.

1. Background

Optically stimulated luminescence (OSL) 'shine plateaux' are plots of equivalent dose (D_e), or sample age, versus OSL measurement time and were first introduced by Huntley et al. (1985). The principal reason for plotting OSL data in this manner is to exploit the possibility of accessing electron traps of differing optical stability in order to determine the degree of optical signal resetting prior to burial. It has been suggested (e.g. Huntley et al., 1985) that data showing a rise in D_e as a function of measurement time may be indicative of insufficient signal resetting prior to deposition. A second consideration is that of the relative thermal stability of different portions of the OSL signal. A signal comprising components of significantly different thermal stability would be expected to yield an age estimate that was dependent upon measurement time if the burial period was significant and fading of part of the signal had occurred. This paper addresses only the issue of optical stability however, focusing on the potential identification of partially bleached quartz samples. Given that only a fraction of D_e versus measurement time plots yield true (flat) 'plateaux', the more general term '$D_e(t)$-plot' will be used henceforth in preference to 'shine plateau' as the generic name for such plots.

It has become fairly common practice to construct OSL $D_e(t)$-plots and a number of such plots can be found in the literature. However, many authors have commented on the lack of understanding of the various forms obtained when OSL data are plotted in this way [see for example Rhodes (1988), Berger and Huntley (1994), Wood (1994), Perkins and Rhodes (1994)] and a variety of both 'rising' and 'falling' forms have been reported. Roberts et al. (1994) investi-

E-mail address: richard.bailey@rlaha.ox.ac.uk (R.M. Bailey).

1350-4487/00/$ - see front matter
PII: S1350-4487(99)00256-5

gated the rising $D_e(t)$-plot data from their Australian quartz samples and found no explanation of the form in either incorrect background subtraction or inappropriate growth-curve fitting. Further they suggested incomplete bleaching prior to deposition is also not sufficient to account for their observations. This latter argument is based on evidence of bleaching taken from the TL plateau data, quoted to be flat over the range 270–430°C, where electron traps of differing sensitivities to bleaching were expected to have influence (Roberts et al., 1994). Examination of these TL plateau data (Fig. 5 of Roberts et al., 1994) however shows there to be a noticeable drop in D_e estimates in the 325°C TL region, where it may be argued that the most bleachable electron traps would dominate. Roberts et al. (1994) propose that the explanation for their observations is that rising $D_e(t)$-plots are an inevitable consequence of interactive (non-first-order) kinetics during optical depletion/measurement. This assertion is examined further in Section 2.1.

A fundamental requirement for the plateau test, if it is to be a useful tool employed in the detection of partially bleached sediments, is that plateaux (i.e. constant D_e with illumination time, in other words a flat $D_e(t)$-plot) should be observed for samples known to have been fully depleted of OSL prior to burial/irradiation. The present investigation addresses this issue, focusing specifically on two factors regarded as being particularly significant: (i) charge phototransfer during OSL measurement; and (ii) the composite nature of the quartz OSL signal (Bailey et al., 1997). In the following section (Section 2) theoretical aspects associated with (i) and (ii) above are examined. The investigation is continued in Section 3 where a series of laboratory measurements are reported. This work relates specifically to quartz OSL although in principle, generalizations to other mineral types may be possible.

2. Theoretical aspects

2.1. The effect of phototransferred charge

Both Bailey (1997, 1998) and Wintle and Murray (1997) provide evidence that charge transferred to the 110°C TL region during room temperature OSL measurements is optically unstable. An optical half-life of ~500 s was calculated by the present author (Bailey, 1997) for the conditions described in Section 3 (room temperature illumination). Clearly the addition of such a component to the observed OSL will affect the OSL decay form (see McKeever et al., 1997) and therefore possibly the form of the $D_e(t)$-plot. The effect is likely to be influenced by a variety of factors, including the level of trap occupancy at the onset of illumination; the charge transfer efficiency; the relative concentration and saturation levels of the OSL and 110°C PTTL traps; the illumination wavelength; and the measurement temperature. In order to assess quantitatively the likely effect of PTTL on the OSL decay form, numerical simulations of a simplified electronic system analogous to that of quartz were used. Fig. A1 is an illustration of the simulated electronic system. Brief details of the model, including the rate equations and simulation sequence (Fig. A2), are given in Appendix A.[1] The parameters of the model (see Table 1) were constrained through comparison of the simulated data to that derived empirically from laboratory measurements. In the comparison (that included TL and OSL growth characteristics, charge transfer efficiency and some aspects of sensitivity change) the simulated data matched very closely those observed experimentally (see Bailey, 1998 for full discussion). Note that there is only one primary optical donor level in this model (Trap 2) and that charge re-trapping is permitted. The 110°C TL trap equivalent (Trap 1) is also bleachable in accordance with the findings of Bailey (1997), having an optical half-life of ~500 s under the simulation conditions described in Appendix A (for $T = 20$°C). As Trap 1 is emptied during preheating, and populated only by photo-transferred charge during illumination at < 110°C, it is not a primary optical donor level.

Fig. 1 shows data from simulations of OSL measurements made at 20°C and 160°C. At 20°C, during which time a portion of the optically detrapped charge is captured at Trap 1, the decay form is clearly affected, both by the 'secondary' OSL (from Trap 1) and also the phosphorescence from Trap 1. Consequently, D_e estimates calculated as a function of measurement time are shown to rise (by ~6%, see Fig. 1(i)). Similar data for a simulated 160°C measurement (where, due to thermal detrapping, there is no net storage of charge in the 110°C TL trap, Trap 1) show no such rise. The OSL decay form at 160°C is well fitted with a single exponential decay, lending support to the findings of Bailey et al. (1997), who show analytically that exponential decay is expected under conditions similar to those modelled in Fig. 1(ii). Minor dose dependent deviations away from a single exponential (maximum deviation being $< 1\%$) are apparent in the simulated OSL data however and consequently the $D_e(t)$-plot form is affected to a small degree. These effects are minor and the overall form of the simulated $D_e(t)$-plot is flat. There is no significant difference in

[1] The model described in Appendix A [similar to that used by McKeever et al. (1997), but with optical stimulation from Trap 1 allowed] is a gross simplification of the electronic system of quartz, though sufficient for the present exercise. Further development of this model has been undertaken and the results of this work will be presented elsewhere.

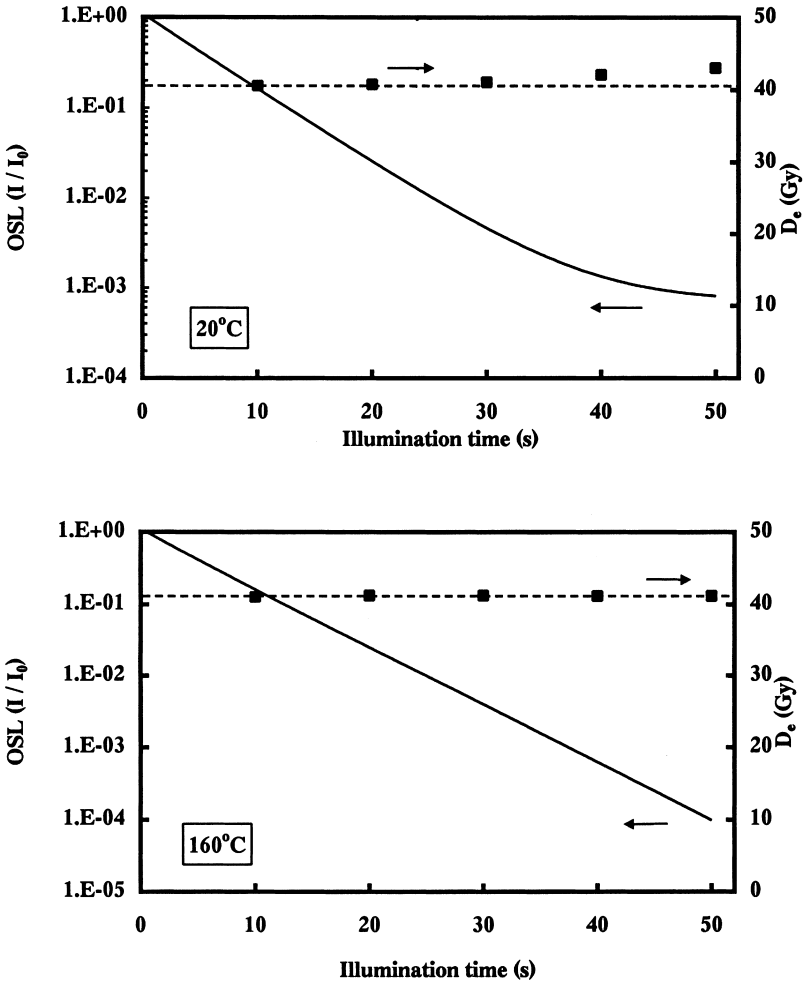

Fig. 1. Results from the simulation described in Appendix A. The upper and lower parts show data from the 20°C and 160°C OSL simulations respectively, normalized to unity at $t = 0$. D_e estimates are in units Gy (simulated). The horizontal dashed line on each fig. represents the D_e estimate from the full integral of the simulated OSL measurement.

the estimate of D_e between any of the points derived from the simulated 160°C OSL (see Fig. 1(ii)); this is not the case for the 20°C data (see Fig. 1(i)).

Table 1
Numerical values used in solving Eqs. (1) and (2), for both Case 1 (the 'typical' case) and Case 2 (the 'extreme' case)

Case 1	λ (s^{-1})	D_0 (Gy)	N (A.U.)
Fast	0.110	100	600
Medium	0.029	500	100
Ratio (F/M)	3.793	0.200	6.000
Case 2	λ	D_0	N
Fast	0.110	100	500
Medium	0.029	500	500
Ratio (F/M)	3.793	0.200	1.000

The rise in D_e through illumination time in the 20°C data is not large, however, and is only apparent following depletion to low signal levels (< 1% of initial intensity). The effect was found to be sensitive to the chosen value for the transition probability A_1 (see Appendix A). Increasing this value by sufficient amounts to yield a significant rise in D_e through illumination time (an increase in A_1 by a factor of ten) gives unrealistically high levels of phototransfer (to Trap 1) compared to empirical measurements in quartz. The rise in the simulated $D_e(t)$-plot due to the effects of charge phototransfer to the 110°C TL region is therefore regarded as being minimal. In quartz samples illuminated at relatively low temperatures (< 110°C), the effect is likely to be similarly small though possibly not insignificant if the concentration of 110°C PTTL traps is proportionately higher than in the current simulation

case. The following section concentrates on dose response factors and suggests these may have a far greater impact on the form of the $D_e(t)$-plot than the effects of PTTL.

2.2. Multiple OSL components

Bailey et al. (1997) and Bailey (1998) show that much of the change in OSL decay form observed following partial bleaching and also following irradiation can be understood in terms of a model in which the OSL measured at 160°C comprises three separate components, each having different growth characteristics and optical stability. It has been demonstrated that the ratio of the first two (most rapidly bleached) components (both of which decay exponentially under optical stimulation, named the 'Fast' and 'Medium' components respectively) is significantly affected by bleaching history. Both the form and the magnitude of the third 'slow' component signal are affected by partial bleaching (Bailey, 1998). The dependence of decay form on prior partial bleaching, and the subsequent record of this change observed following additional irradiation (Bailey et al., 1997), suggests that information relating to bleaching history may indeed be available through examination of the OSL decay form and that the $D_e(t)$-plot may be a possible means of accessing this information. Of course, in light of the findings presented in Section 2.1, the use of raised temperature OSL measurements may be preferable in order to remove the effects of phototransferred charge. Complication arises however when consideration is made of differences in the dose response of each OSL component (see Bailey et al., 1997; Bailey, 1998). Such differences may affect the form of the $D_e(t)$-plot, even in cases where the origin for the growth function of each component is common, at zero (i.e. where the signal from each component has been fully removed prior to signal growth), as a result of dose dependent variation in the proportional contribution of each component to the total signal at a given time.

It is common practice to employ single saturating exponential fits in order to describe, and extrapolate beyond, OSL dose response data. Clearly, for samples possessing multiple constituent OSL components (each having different saturation levels) this practice will yield both inaccurate estimates of D_e from the full integral OSL data and is also likely to produce a variety of $D_e(t)$-plot forms. The exact shape of such plots will depend on the relative magnitudes, growth rates and saturation levels of the components present. The remainder of this Section (2.2) documents an attempt to investigate, theoretically, the possible effects on $D_e(t)$-plot form of multiple constituent components, each with different dose saturation characteristics. The influence of optically unstable phototransferred charge, as described above, is not included in this section of the investigation, both for ease of interpretation and because for quartz (as reported in Section 2.1) the effect is likely to be minor.

The simplified model (Eqs. 1 and 2) describes a signal comprising only two separate components (i.e. a fast and a medium component), each decaying exponentially under optical stimulation. In the samples measured to date (see Bailey, 1998), these two components are responsible for the majority of the signal observed over a duration sufficient to reduce the OSL to ~5% of the initial intensity and so contribute most of the signal used in the construction of OSL $D_e(t)$-plots.

The total OSL signal (at time t), following dose $D+\beta$ is defined

$$\mathrm{OSL}(t) = \left[\mathrm{OSL_F}(t) + \mathrm{OSL_M}(t)\right], \tag{1}$$

where the signal from each component (**F**ast and **M**edium) is given by

$$\mathrm{OSL}_i(t) = \left[N_i(1 - \exp\{-(D + \beta)/D_{0i}\})\lambda_i \mathrm{P}\right] \exp(-\lambda_i t). \tag{2}$$

For each of the signal components $i=F$ and $i=M$, N_i = maximum trapped electron concentration (cm^{-3}); D_{0i} = constant (dose at which the slope of the dose response is equal to 1/e of the initial value) (Gy); D = burial dose (Gy);[2] β = laboratory dose, added for growth curve construction (Gy); λ_i = optical detrapping constant (s^{-1}); P = proportion of detrapped charge that undergoes radiative recombination (constant, at unity, throughout illumination);[3] t = illumination time (s).

The first term of Eq. (2) (in square brackets) gives the expression for growth due to irradiation (natural plus laboratory), multiplied by the optical depletion constant λ_i to yield OSL intensity at $t = 0$. The second term describes the exponential decay of the OSL during measurement.

Two cases were simulated, each having a different proportion of fast to medium component signals. For each of these cases, the numerical parameters used to solve Eq. (2) are presented in Table 1. Note that values

[2] For the purpose of this work, D represents the known burial dose. The term D_e refers to the estimate of dose D derived from the OSL measurement (simulated or measured empirically).

[3] For many samples the loss of sensitivity (as measured using the 110°C TL response to a small β test dose) through illumination (420–560 nm) is between 0 and 10%. Setting P constant is therefore a simplification though the effect is negligible.

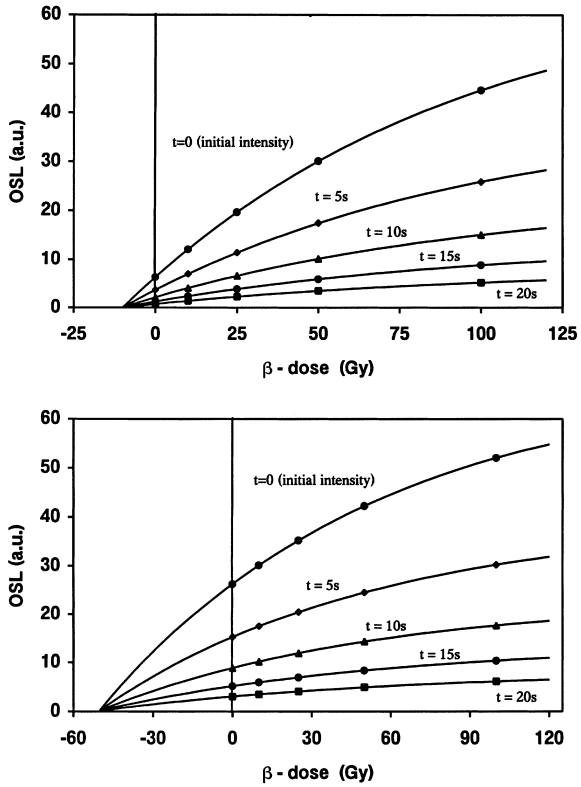

Fig. 2. Example of the simulated OSL growth curves produced using Eqs. (1) and (2). Data shown are for Case 1, $D = 10$ Gy and $D = 50$ Gy (see Tables 2 and 3 for further information). The range of the data shown is limited to the added dose range 0–100 Gy in order to show the detail near the intercept. For fitting (D_e calculation) the range 0–300 Gy (added dose) was used, as described in the main text.

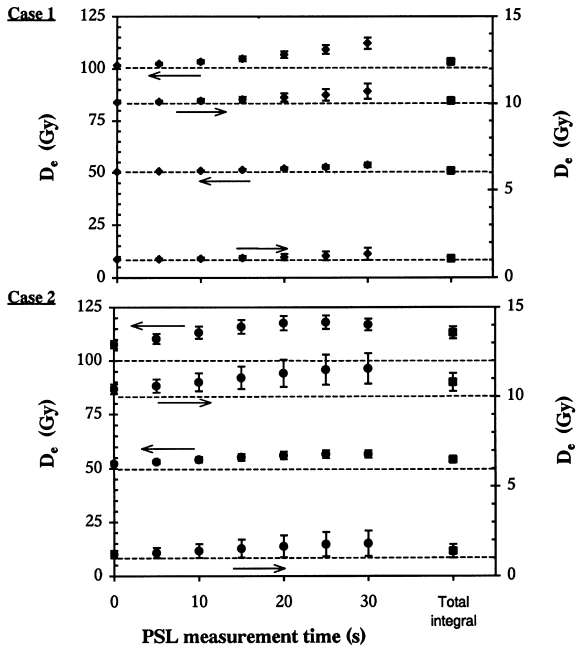

Fig. 3. $D_e(t)$-plots constructed from numerical data produced by Eqs. (1) and (2) (Case 1, above; Case 2, below). Dotted lines indicate the 'given dose' D for each data set, with arrows pointing to the appropriate dose (D_e) axis.

of N are unrealistically small, having been scaled down for ease of handling. This scaling has no effect on the form of the final results. Note also that no remnant signal due to partial bleaching is included in the present simulations. The total dose accumulated in each component is simply $D+\beta$ and is therefore identical for both signal components. The relative optical decay rates of the fast and medium components are identical for both cases and reflect the depletion rates observed for the fast and medium OSL components under the conditions described in Section 3, for $T = 20°C$. The difference in relative signal magnitude ($N_F/N_M = 6$ for Case 1; $N_F/N_M = 1$ for Case 2) represents (i) a typically observed (saturated) fast/medium component ratio (Bailey, 1998) (Case 1) and (ii) the lowest fast/medium component ratio observed for quartz (Bailey, 1998) (Case 2). The modelled rate of growth with dose ($D_{0F}/D_{0M} = 0.2$ for Cases 1 and 2) relates to the commonly observed dose response of measured quartz samples (Bailey, 1998). Case 1 therefore reflects the most likely set of parameter for a 'typical quartz sample' and Case 2 sets the likely upper limit of any observable signal component related effect.

For both Cases 1 and 2, results were calculated for a range of different D values: 1, 10, 50 and 100 Gy. Simulated dose response data were fitted to a single saturating exponential (to equally weighted points) over an added dose range (β) of 0–300 Gy, extrapolation to OSL = 0 providing the estimate of D_e (see examples in Fig. 2). $D_e(t)$-plots constructed using Eq. (1), for each case and for each value of D, are shown in Figs. 3(i) and (ii). The data plotted (D_e versus t) cover the 0–30 s measurement period (at 5 s intervals), during which time (the modelled) OSL intensity reached a level of ~6% that at $t = 0$ (the precise level depending upon N_F/N_M, D_{0F}/D_{0M} and $D+\beta$. This level of OSL was considered representative of the lowest level from which measured quartz OSL data could be distinguished reliably from background (including slow component contributions) in order to construct a meaningful $D_e(t)$-plot.

The model (Eqs. 1 and 2) yields $D_e(t)$-plots for both Case 1 and 2 that rise with measurement time. For Case 1 (the 'typical sample') the D_e (t)-plot is relatively flat for low values of D (i.e. in the region where OSL ($F+M$) response is approximately linear with dose). As D increases, the degree of deviation from the (flat) 'plateau' increases also, the effect of the difference in

Table 2
Numerical summary of the changes in simulated D_e as a function of OSL measurement time

	D_e (Gy)			
D (Gy)	$t = 0$ s	$t = 30$ s	Difference	% difference
Case 1				
1	1.04	1.35	0.31	29.81
10	10.08	10.71	0.63	6.25
50	50.44	53.66	3.22	6.38
100	101.57	112.15	10.58	10.42
Case 2				
1	1.2	1.81	0.61	50.83
10	10.42	11.57	1.15	11.04
50	52.28	56.65	4.37	8.36
100	107.72	116.93	9.21	8.55

D_0 between each component being accentuated as saturation is approached. Table 2 gives a brief summary of the results obtained, comparing D_e at $t = 0$ s and t = 30 s. The difference between D_e at $t = 0$ s and t = 30 s is greater (in absolute terms) for larger D in both Case 1 and 2. By proportion, the trend is not so clear and depends upon the chosen parameters. Table 3 provides a summary of the 'total integral' data, comparing D to D_e. For both Cases and for all values of D, D_e is an overestimate, though only by a few percent in Case 1, the 'typical quartz'. For Case 2, the deviation of D_e from D is substantial for all values of D. Table 3 also shows the uncertainty in D_e (both in absolute and percentage terms). The uncertainty associated with each value of D_e arises from the inaccuracy of fitting a single exponential model to data comprising two exponential components. An important question following on from this is whether such inappropriate fitting would be recognizable in empirical data. Given that quartz OSL ('total integral') dose response data commonly yields an inter-aliquot precision of no better than 5% (using multiple aliquot additive dose techniques), the possibility of detecting multiple growth components (such as in Case 1) seems remote. The relatively small errors on D_e (modelled data, Table 3), together with the visually convincing fits presented in Fig. 2, further confirm this view. Attempts to derive the correct D_e (i.e. D) from the data produced using Eqs. (1) and (2) were made using a two-exponential fitting function. As expected, the intercept of the function (at OSL = 0) was in full agreement with the true dose, D, with negligible uncertainty. $D_e(t)$-plots obtained using the 2-exponential fitting procedure yielded constant D_e (equal to D) with illumination time for both cases (also with negligible uncertainty). For (non-perfect) laboratory data, the increased number of fitting parameters required in going from a single to a multi-exponential would dramatically raise the level of uncertainty on the estimate of D_e. Nonetheless, the 2-exponential fit appears in the case of the modelled data to give correct estimates of D_e. An obvious remedy to the problem of larger statistical uncertainty on D_e is to increase both the number and range of data points used.

It is worth underlining that the simulations described above are of fully reset samples (i.e. the dose in each component is identical) and that the introduction of partial bleaching into the results would complicate matters further. However, the purpose of the present study, as stated in Section 1, was to assess the form of $D_e(t)$-plots from fully zeroed samples, the condition of constant D_e with illumination time being the fundamental requirement under investigation. A variety of $D_e(t)$-plot forms can be obtained by fitting a single saturating exponential to data produced using Eqs. (1) and (2). Depending upon the choice of parameters (within realistic limits) the $D_e(t)$-plots exhibit relatively flat, rising, falling and peaked forms.

3. Laboratory measurements

Laboratory simulations were undertaken in order to test empirically the theoretical findings of the previous two sections. A single quartz sample was used for lab-

Table 3
A summary of both the accuracy and precision of D_e estimates obtained using data produced by Eqs. (1) and (2)

	$D = 1$	$D = 10$	$D = 50$	$D = 100$
Case 1				
D_e (Gy)	1.08	10.17	50.95	103.33
Error on D_e [%]	0.08 [7.4]	0.11 [1.08]	0.32 [0.63]	0.85 [0.82]
% deviation from D	8.00	1.70	1.90	3.33
Case 2				
D_e (Gy)	1.38	10.8	54.14	113.19
Error [%]	0.38 [27.5]	0.50 [4.63]	1.28 [2.36]	2.84 [2.51]
% deviation from D	38.00	8.00	8.28	13.19

oratory experiments: 90–125 μm quartz grains extracted from modern beach sand (Eastbourne, UK), annealed in air at 580°C for 40 min (henceforth EBSan). An annealed sample was used for two reasons: (i) to ensure the signal level was minimal at the onset of irradiation; and (ii) to increase the signal-to-noise ratio (although unfortunately the scatter in the results remained at a higher level than that expected).[4] The use of an annealed sample does of course detract from the confidence with which any conclusions drawn from these measurements can be generalized to natural sedimentary quartz. However, the departure from generality is not expected to be so significant as to negate completely the usefulness of the experiment given that both the optical depletion rate (of the fast and medium OSL components) and rate of growth with dose is unaffected by the annealing treatment.

All measurements were made on an automated Risø set (TL-DA-12), using a 75 W filtered halogen lamp light source, stimulating in a band between approximately 420 and 560 nm (2.21–2.95 eV, nominally 16 $mW.cm^{-2}$ at the sample [see Bøtter-Jensen and Duller (1992) for details]. Filtering of the halogen lamp was with a single HA-3 heat absorbing filter, 9 mm of GG420 glass filters and a broadband interference filter (Bøtter-Jensen and Duller, 1992). Emissions were filtered in all cases with 5 mm of U340 glass filters. An EMI 9635QA photo-multiplier fitted with a bialkali cathode was used for photon counting.

For the first experiment, two batches of sample aliquots were mounted on to stainless steel discs using viscous silicone oil and β-irradiated with standard doses: 10 Gy (batch 1); 43 Gy (batch 2). All aliquots were subsequently preheated at 220°C for 300 s prior to a normalization OSL measurement lasting 0.1 s (at 20°C). Following this, additive β-doses and a second identical preheat were administered to each batch of discs. OSL measurements were finally made at 20°C. Infrared stimulation was used both before and after each irradiation stage in order to screen for possible feldspar contamination (Spooner and Questiaux, 1989). The measured signal was indistinguishable from the background.

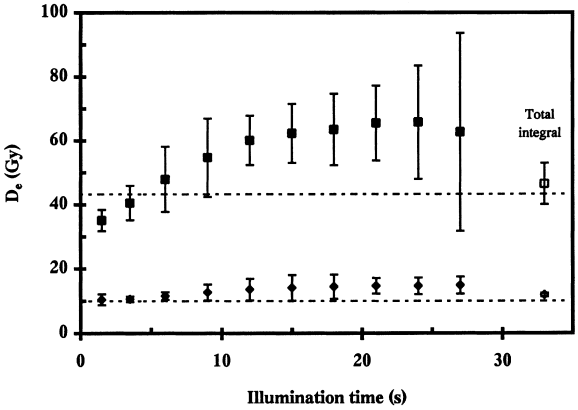

Fig. 4. $D_e(t)$-plots from laboratory simulations, using sample EBSan with a given standard β-doses (D) represented by horizontal dashed lines. The total integral D_e estimate is also shown. See main text for further details.

$D_e(t)$-plots derived from these measurements are shown in Fig. 4 (each point being the integral over the preceding 1.5 s of illumination). Following administration of a 10 Gy dose (i.e. $D = 10$), the resultant $D_e(t)$-plot shows a small rise over the 0–30 s illumination interval. The magnitude of uncertainty at each point is relatively large however and though the overall trend is an upward one, only a small number of points are significantly greater than the initial point. The total integral growth curve in this case gives only a slight overestimate of the administered dose ($D = 10$; $D_e = 11.85 \pm 0.56$ Gy). For $D = 43$ Gy, the rise in D_e is far more dramatic and the majority of points have greater values than the initial point (at $t = 1.5$ s). These findings match with those of the previous Section (2.2) in that the degree of deviation from constant D_e (as a function of illumination time) is greater as D increases — the form of the response being intermediate between Cases 1 and 2. D_e based on the total integral measurement is in this case indistinguishable from the administered dose ($D_e = 46.45 \pm 6.44$ Gy).[5]

A repeat measurement was made of the higher dose condition, measuring OSL at 160°C in order to remove potential effects of PTTL described in Section 2.1. A shorter measurement time and lower excitation power (~8 $mW.cm^{-2}$) were used to counteract the faster OSL depletion rate at 160°C compared to 20°C (reduction over 20 s at 160°C being to ~0.5% of I_0). The results of this experiment are shown in Fig. 5. Clearly, all points (including the 'total integral') lay above the level D (the administered dose). This pattern of results (a 'rising form' where each data point lies above the

[4] These experiments were attempted a number of times using daylight bleached natural sedimentary quartz (i.e. non-annealed). In every case the scatter observed between aliquots precluded meaningful fitting and it was only after several such attempts that the decision was made to use an annealed sample.

[5] The high count rate observed during this measurement may have caused a degree of 'pile-up' in the photomultiplier. This effect has not been corrected for. Determining the precise effect of signal pile-up on the form of the $D_e(t)$-plot is not straightforward but may help to explain the unexpectedly low values of D_e calculated from the initial (highest count rate) region of the OSL decay (the effect of course being greater for higher doses, potentially increasing the degree of sub-linearity in the dose response curve and thus reducing D_e).

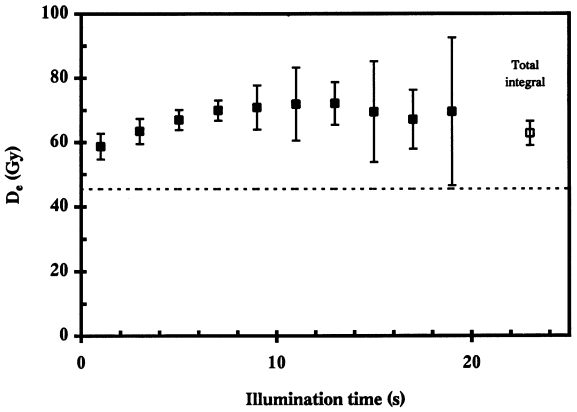

Fig. 5. $D_e(t)$-plots from laboratory simulations, using sample EBSan with a given standard β-dose (D) represented by the horizontal dashed line. The total integral D_e estimate is also shown. See main text for further details.

administered dose, D) is similar to that predicted by Eqs. (1) and (2) (Section 2.2) for Case 2 (see Fig. 3). However, the magnitude of D_e overestimation observed empirically (Fig. 5) is significantly greater than that predicted by the model. The model [Eqs. (1) and (2) of Section 2.2] is therefore clearly insufficient in its present form to account for the 160°C data. This matter is discussed directly below.

Precise modelling of the observed OSL from sample EBSan (with regard to the proportional contribution of fast, medium and slow components) was not possible owing to uncertainties in the form of slow component OSL decay. The observed form of OSL decay ('bulk' signal) was visually similar to the vast majority of samples measured previously (see Bailey, 1998) and there is no reason to believe OSL from this sample is significantly different in fast/medium component composition to that encompassed in the range of 'typical' (Case 1) to 'extreme' (Case 2) samples previously described in Section 2.2. An explanation of the strong effect observed in Fig. 5 must therefore be sought.

One possibility is that the growth rate (during irradiation) of the fast and medium OSL components of sample EBSan are significantly different from those modelled (Cases 1 and 2, see Table 1). Varying the filling rate of each component would clearly affect the $D_e(t)$-plot although without additional work it is difficult to predict the precise effect and this possibility has not been investigated further.

Erroneously large values of D_e may occur if insufficient background is subtracted from the raw OSL data. Although a plausible explanation for data of the form is presented in Fig. 5, it is unlikely that this is the case for Fig. 5. Initial OSL intensity measured during illumination was of the order of millions of counts per second, depending upon the added dose. Any errors associated with incorrect background subtraction (background being ~200 cps) would therefore have had a negligible effect on the D_e (t)-plot data, given the magnitudes involved. More likely is that the presence of the 'slow component' (Bailey et al., 1997) affected the $D_e(t)$-plot data at relatively low signal levels [this was not accounted for in Eqs. (1) and (2)]. Given the gradual bleaching rate of the slow component, it is to a good approximation a constant-level signal over short (in this case 20 s) duration measurements. A relatively large slow component would therefore be equivalent to subtracting too little background from the measurements and this may account for the results shown in Fig. 5.

An additional point is that thermal assistance (in the detrapping process; Bailey, 1998) may have exaggerated the contribution from the slow component in the 160°C data. Very little slow component signal is observed at 20°C whereas at 160°C the signal is clearly present. A further possibility is that thermal quenching (at 160°C) affects the slow component less than the fast and medium components, leading also to a signal comprising proportionately of a more slower component at 160°C than at 20°C. It is worth noting also that a number of other possible contributory factors (such as the effects of thermal transfer (Rhodes and Bailey, 1997) and sensitivity change) may affect the laboratory measured OSL and lead to erroneous D_e estimates. These effects would be similar for both the 20°C and 160°C data, however they are not included in either of the present simulations.

If data such as in Fig. 5 were obtained for a 'known age' sample (i.e. equivalent to a sample with a known value D, given that the natural dose rate was well defined) a simplistic interpretation would be that the significant overestimate of age (total integral estimate), accompanied by the rising $D_e(t)$-plot, was strong evidence for the sample having been only partially bleached prior to burial. As such, this would add weight to the notion that rising $D_e(t)$-plots are good indicators of partial bleaching. If total integral overestimates of D are commonly associated with rising $D_e(t)$-plots (as suggested by Cases 1/2 and by Figs. 4 and 5) it is clear to see how the apparent connection between incomplete resetting and $D_e(t)$-plot form could continue to have been made.

Attempts at fitting a two-exponential function to the dose response data obtained empirically (those used for the construction of $D_e(t)$-plots given in Figs. 4 and 5) yielded unreliable results. As mentioned towards the end of Section 2.2, relatively large numbers of data points are required before statistical uncertainties on such functions (even with relatively precise data) are reduced to useful levels. Further measurements are therefore required and at present the issue of multi-ex-

ponential fitting (for the purpose of $D_e(t)$-plot construction) remains unclear.

4. Conclusions

Results of numerical modelling suggest that PTTL may affect the form of $D_e(t)$-plots in cases where OSL measurements are made at temperatures that allow net storage of charge in the trap(s) responsible for the '110°C' TL peak. Further complications may occur due to differences in the dose response characteristics of each constituent OSL signal component (see Fig. 3) where single-saturating-exponential fitting is employed. In such cases, the degree of deviation from constant D_e (through measurement time) may increase with palaeodose. Empirical measurements reported in Section 3 are consistent with these theoretical findings. This is an unfortunate finding as far as multiple-aliquot optical dating is concerned as it calls into question the validity of interpretations based on the structure of $D_e(t)$-plot data. For the sample used (see previous section), the first and most fundamental requirement of the plateau test has not been met. A (flat) plateau was not obtained from a sample known to have been fully reset prior to irradiation. Stokes (1994, Appendix H) shows data from measurements of a sample containing intentionally partially bleached grains. Plots of D_e versus measurement time in that case yielded a flat $D_e(t)$-plot and hence no indication of the known prior partial bleaching. Together, these two findings suggest that routine use, for all quartz samples, of the so-called OSL 'shine plateau' test, as a means of identifying partially bleached sediments, is not straightforward. Other samples must of course be investigated in this manner before wider generalizations can be made. However, that even some samples can fail such rudimentary tests is not encouraging.

Without sufficient quantification of the dose response of different sections of the OSL decay curve (i.e. the different OSL signal components), use of the 'shine plateau' test is perhaps best suited to the analysis of raised temperature measurements of samples that have not been irradiated to high doses (either naturally or in the laboratory). What is meant by 'high dose' is, of course, likely to be sample dependent but in this context it refers to the dose required to induce significant sub-linear growth in any of the signal components. The question of which part of the 'bulk' signal is best able to provide the 'correct' D_e is difficult to answer, likely as it is to be sample dependent. Based on the evidence from this investigation, the total integral D_e appears to be the most reliable option. In previous studies (e.g. Stokes, 1994) the ages derived from total integral OSL measurements have been found to be reliable, agreeing in most cases with independent age controls.

Consideration of the composite nature of the quartz OSL signal (Bailey et al., 1997; Bailey, 1998) suggests that partial bleaching may indeed be detectable through examination of the OSL decay form. An alternative to potentially problematic examinations of the 'bulk' OSL signal is to examine the individual signal from each OSL component. Such an investigation requires only that OSL measurements are made at raised temperatures over an extended duration (in order to reliably separate the individual signal components; Bailey, 1998) and offers a means of assessing the dose response of each OSL component and hence the utility of the D_e (t)-plot. Bailey et al. (1997) present a potentially useful method of detecting partially bleached samples, based specifically on the analysis of the fast and medium OSL signal components.

This work relates only to the multiple-aliquot method of D_e determination and the use of single aliquot techniques has not been discussed. Modelling of single aliquot regenerative methods (plotting D_e as a function of measurement time) in order to assess the potential for partial bleaching detection is currently underway and early results suggest the use of $D_e(t)$-plots may in fact be well justified (flat and rising $D_e(t)$-plots being expected for well bleached and partially bleached samples respectively). A full discussion of the analysis of $D_e(t)$-plots obtained from single aliquot measurement procedures will be presented elsewhere.

Acknowledgements

I am grateful to Professor Ann Wintle, Dr. Barnaby Smith, Dr. Stephen Stokes and those at the Research Laboratory for Archaeology and the History of Art (Oxford) for helpful discussion and comments on various versions of this manuscript.

Appendix A. Details of the numerical model

Listed below are the equations used to describe the charge transitions shown schematically in Fig. A1

Optically and thermally unstable electron trapping centres [Levels 1 & 2]:

$$\mathrm{d}n_i/\mathrm{d}t = \Sigma(-n_i \cdot g_i - n_i \cdot s_i \cdot \exp(-E_i/k_b \cdot T) + n_c \cdot (N_i - n_i) \cdot A_{ni}) \quad (i = 1, 2) \tag{A1}$$

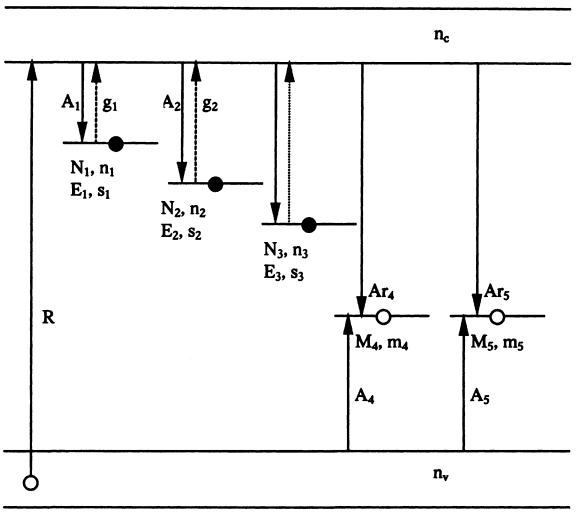

Fig. A1. A band diagram representation of the modelled electronic system. All allowed transitions of charge within the system are shown, with movement indicated by arrows. The small dashed arrow (arr) represents thermal detrapping only of electrons (from level 3); the large dashed arrow (– – – –▶) represent thermal and optical detrapping of electrons (from trapping levels 1 & 2). Other symbols are as listed in Appendix A.

Optically stable, thermally unstable electron trapping centres [Level 3]:

$$\mathrm{d}n_j/\mathrm{d}t = -n_j \cdot s_j \cdot \exp(-E_j/k_b \cdot T) + n_c \cdot (N_j - n_j) \cdot A_{nj} \quad (j = 3) \tag{A2}$$

Radiative hole centres [Level 4]:

$$\mathrm{d}m_l/\mathrm{d}t = n_v \cdot (M_l - m_l) \cdot A_{ml} - n_c \cdot m_l \cdot A_{rl} \quad (l = 4) \tag{A3}$$

Non-radiative hole centres [Level 5]:

$$\mathrm{d}m_k/\mathrm{d}t = n_v \cdot (M_k - m_k) \cdot A_{mk} - n_c \cdot m_k \cdot A_{rk} \quad (k = 5) \tag{A4}$$

Conduction band population:

$$\mathrm{d}n_c/\mathrm{d}t = R + \Sigma\{n_j \cdot s_j \cdot \exp(-E_j/k_b \cdot T) - n_c \cdot (N_j - n_j) \cdot A_{nj}\} + \Sigma\{n_i \cdot g_i + n_i \cdot s_i \cdot \exp(-E_i/k_b \cdot T) - n_c \cdot (N_i - n_i) \cdot A_{ni}\} - \Sigma\{n_c \cdot m_l \cdot A_{rl}\} - \Sigma\{n_c \cdot m_k \cdot A_{rk}\} \tag{A5}$$

Valence band population:

$$\mathrm{d}n_v/\mathrm{d}t = R - \Sigma\{n_v \cdot (M_l - m_l) \cdot A_{ml}\} - \Sigma\{n_v \cdot (M_k - m_k) \cdot A_{mk}\} \tag{A6}$$

Temperature:

$$\mathrm{d}T/\mathrm{d}t = \beta \tag{A7}$$

Luminescence:

$$\text{Luminescence} = n_c \cdot A_{rl} \cdot m_l \tag{A8}$$

where, $N_{i,j}$ = concentration of electron traps (traps.cm^{-3}); $n_{i,j}$ = concentration of trapped electrons (electrons.cm^{-3}); $s_{i,j}$ = frequency factors (s^{-1}); $E_{i,j}$ = electron trap depth (eV); $M_{l,k}$ = concentration of hole traps (traps.cm^{-3}); $m_{l,k}$ = concentration of trapped holes (holes.cm^{-3}); k_b = Boltzmann's constant (eV.K^{-1}); T = absolute temperature (K); $A_{ni,j}$ = conduction band to electron trap transition probability (s^{-1}); $A_{ml,k}$ = valence band to hole trap transition probability (s^{-1}); $A_{rl,k}$ = conduction band to hole trap transition probability (s^{-1}); g_i = optical detrapping rate (s^{-1}); β = rate of change in temperature (K. s^{-1}); R = ionisation rate (electrons/holes.s^{-1}); t = time (s).

During Irradiation: $g_1 = g_2 = 0$, $T_0 = 293$, $\beta = 0$, $R = 5 \times 10^8$;

During TL/Preheat: $R = 0$, $g_1 = g_2 = 0$, $T_0 = 293$, $\beta = 5$;

During OSL: $R = 0$, $g_1 = 0.002$, $g_2 = 0.2$, $T_0 = 293$ or 433, $\beta = 0$.

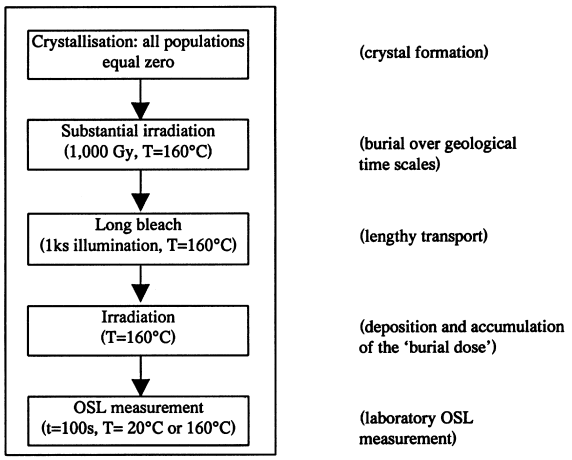

Fig. A2. An illustration of the simulation procedure. Note that following each simulation a 2 s pause at constant temperature was simulated in which valence and conduction band populations reached equilibrium (zero population in the case of the valence band). T = temperature (°C).

Table A1
Table A1 lists the numerical values for each of the parameters defined in Appendix A. Numerical solutions to Eqs. (A1)–(A8) were found using a Runge–Kutta routine. Custom written software was used to perform the numerical calculations (see Bailey, 1998)

Trap	N or M (cm^{-3})	$A_{n,m}$ (s^{-1})	A_r (s^{-1})	E (eV)	s (s^{-1})
1	1×10^{8}	1×10^{-8}	–	0.97	5×10^{12}
2	1×10^{9}	1×10^{-9}	–	1.60	1×10^{13}
3	5×10^{10}	1×10^{-10}	–	1.80	1×10^{10}
4	5×10^{10}	1×10^{-9}	5×10^{-10}	–	00
5	5×10^{10}	1×10^{-10}	1×10^{-10}	–	–

Other numerical values used in the calculations are given in Table A1. The simulation procedure is indicated in Fig. A2.

A1. Notes on the numerical simulation procedure

1. The values chosen for g_1 and g_2 yielded OSL and TL depletion rates (under illumination) equivalent to those typically observed empirically for quartz using the standard Risø-set conditions described in Section 3, i.e. stimulating between ~420 and 560 nm at ~16 $mW.cm^{-2}$ (discussed in Bailey, 1998).
2. Following each simulated treatment (e.g. irradiation, illumination or heating) a 'pause' at constant temperature was simulated, where the conduction and valence band populations were allowed to reach equilibrium (zero in the case of the valence band) prior to the commencement of the next step. A two-second duration was found to be sufficient and was used in all cases.
3. Irradiation at T = 160°C during both the 'geological' and 'burial' doses was incorporated in order to scale up the rate of thermal eviction so as to be in similar proportion (at the high dose rate used) to charge trapping rates as is the case for lower temperature/low-dose-rate irradiation. Specific investigation of dose-rate related effects was not made in the present study however and the appropriateness of 160°C simulated irradiation has not been fully demonstrated.
4. Preheating following simulated laboratory irradiation was only to 140°C as the only unstable charge trapping centre in the present model is Trap 1, the 110°C TL-centre, and this is empty following heating to 140°C.
5. Both electrons and holes represent 'charge units' (C.U.) within the model. The sum of all population terms therefore provides a measure of the 'charge neutrality' of the system. There should be no departure from neutrality throughout the simulations as initially the electronic system is in balance (electronically neutral) and subsequently for every electron ionised during irradiation a hole is also generated (by definition). An assessment of charge neutrality can therefore be used as a measure of the accuracy of the numerical computation. Throughout all of the simulations reported, charge neutrality, q (where $q = [n_c + n_1 + n_2 + n_3 - m_4 - m_5 - n_v]$) wandered about zero within the range ± 0.01 C.U.. This represents an acceptably low error of approximately 1 in 10^{15} (given that the magnitude of both the positive and negative charge within the system during each simulation was of the order of 10^{13} C.U. — depending of, course, upon the 'history' of the simulated sample and the event being simulated).

References

Bailey, R.M., 1997. Optical detrapping of charge from the 110°C quartz TL region. Ancient TL 15 (1), 7–10.

Bailey, R.M. 1998. The form of the optically stimulated luminescence signal of quartz: implications for dating. Unpublished PhD thesis, University of London.

Bailey, R.M., Smith, B.W., Rhodes, E.J., 1997. Partial bleaching and the decay form characteristics of quartz OSL. Radiat. Meas. 27, 123–136.

Berger, G.W., Huntley, D.J., 1994. Tests for optically stimulated luminescence from tephra glass. Quaternary Geochronology (Quat. Sci. Rev.) 13, 509–511.

Bøtter-Jensen, L., Duller, G.A.T., 1992. A new system for measuring optically stimulated luminescence from quartz samples. Nuclear Tracks and Radiation Measurements 20, 549–553.

Huntley, D.J., Godfrey-Smith, D.I., Thewalt, M.L.W., 1985. Optical dating of sediments. Nature 313, 105–107.

McKeever, S.W.S., Bøtter-Jensen, L., Agersnap Larsen, N., Duller, G.A.T., 1997. Temperature dependence of OSL decay curves: experimental and theoretical aspects. Radiat. Meas. 27, 161–170.

Perkins, N.K., Rhodes, E.J., 1994. Optical dating of fluvial sediments from Tattershall, U.K. Quaternary Geochronology (Quat. Sci. Rev.) 13, 517–520.

Rhodes, E.J., 1988. Methodological considerations in the optical dating of quartz. Quat. Sci. Rev. 7, 395–400.

Rhodes, E.J., Bailey, R.M., 1997. Thermal transfer effects observed in the luminescence of quartz from recent glaciofluvial sediments. Quaternary Geochronology (Quat. Sci. Rev.) 16, 291–298.

Roberts, R.G., Jones, R., Spooner, N.A., Head, M.J., Murray, A.S., Smith, M.A., 1994. The human colonisation of Australia: optical dates of 53,000 and 60,000 years bracket human arrival at Deaf Adder gorge, Northern Territory. Quaternary Geochronology (Quat. Sci. Rev.) 13, 575–583.

Spooner, N.A., Questiaux, D.G., 1989. Optical dating — Achenheim beyond the Eemian using green and infrared stimulation. In: Proceedings of Workshop on Long and Short Range Limits in Luminescence dating. Occasional

Publication 9. Research Laboratory for Archaeology and the History of Art, Oxford.
Stokes, S. 1994. Optical Dating of Selected Late Quaternary Aeolian Sediments From The Southwestern United States. Unpublished DPhil thesis, Oxford University.
Wintle, A.G., Murray, A.S., 1997. The relationship between quartz thermoluminescence, photo-transferred thermoluminescence, and optically stimulated luminescence. Radiat. Meas. 23, 323.
Wood, P.B., 1994. Optically stimulated luminescence dating of a late Quaternary shoreline deposit, Tunisia. Quaternary Geochronology (Quat. Sci. Rev.) 13, 513–516.